

Synthesis and Characterization of Hyperbranched Polyacrylamide Using Semibatch Reversible Addition–Fragmentation Chain Transfer (RAFT) Polymerization

Wen-Jun Wang,^{*,†} Dunming Wang,[†] Bo-Geng Li,[†] and Shiping Zhu^{*,‡}

[†]State Key Laboratory of Chemical Engineering, Institute of Polymerization and Polymer Engineering, Department of Chemical & Biological Engineering, Zhejiang University, Hangzhou, Zhejiang, P.R. China 310027, and [‡]Department of Chemical Engineering, McMaster University, Hamilton, Ontario, Canada L8S 4L7

Received January 29, 2010; Revised Manuscript Received April 2, 2010

ABSTRACT: Hyperbranched polyacrylamides (b-PAM) were synthesized using a semibatch RAFT copolymerization of acrylamide (AM) and *N,N'*-methylenebis(acrylamide) (BisAM) with continuous feeding of BisAM. Small amounts of chain transfer agent (CTA), 3-benzyltrithiocarbonyl propionic acid, with 1/20 to 1/50 molar ratios to BisAM were used to control gelation during the polymerization. Influences of BisAM addition rate, CTA to initiator molar ratio, and AM concentration were also systematically examined. Hyperbranched structures were analyzed by a triple-detector GPC and NMR measurement. The b-PAM polymers had branching densities from 7.2 to 11.7 branches per 1000 carbons, with contraction factors g' of 0.295–0.416 and g of 0.201–0.290, weight-average molecular weights of 5.63×10^5 to 1.28×10^6 g/mol, and polydispersity indexes of 4.7–8.6. It was found that intramolecular cyclization was significant in the polymerization and a substantial number of cyclic structures were formed in the b-PAM samples. Fractionation of GPC traces having the same numbers of primary chains elucidated that branch points were randomly distributed along primary chain backbones. The semibatch process with combined use of BisAM and CTA provided an effective approach to prepare the b-PAM samples at high conversion under low CTA usage.

Introduction

Highly branched polymers have been used in drug delivery systems, catalyst supports, viscosity modifiers, etc. Their applications have been extended lately into the areas of nanotechnology and biomedicine.^{1,2} Among various highly branched polymers, acrylamido polymers have received much attention due to their hydrophilicity and stimuli-response.^{3–8}

As a type of branched polymers, dendrimers have a well-controlled branched structure and have been intensively studied for more than 2 decades.⁹ However, their applications have been limited due to difficulties in preparation. Hyperbranched polymers, as a type of dendritic polymers,² offer an alternative, and they have been studied in recent years.^{1,2,9,10} Although not as well controlled as dendrimers, synthesis of hyperbranched polymers is much easier and more cost-effective.^{1,2,10–13}

In the early years, hyperbranched polymers were normally synthesized by step-growth polymerization of AB_n type of monomers through reaction between A and B. Frechet et al.¹⁴ first introduced a self-condensing vinyl polymerization (SCVP) to prepare hyperbranched vinyl polymers using an AB vinyl monomer with functional group B for successively initiating polymerization of vinyl group A. The SCVP approach was further adopted and combined with controlled/living radical polymerization for synthesis of hyperbranched polymers. Matyjaszewski et al.^{15–19} and Muller et al.^{20,21} used this approach to prepare hyperbranched structures via atom transfer radical polymerization (ATRP) of AB-type styrenic or acrylic monomers. Functional group B acted as an initiating moiety for consecutive ATRP. Hawker and Frechet et al.¹¹ used nitroxide-mediated polymerization (NMP) to

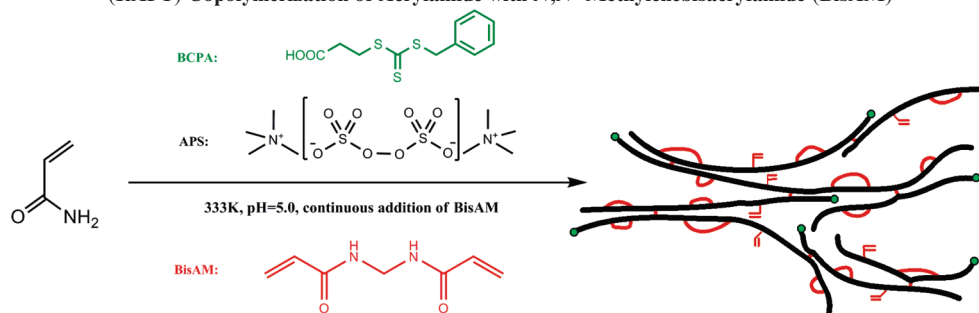
synthesize a hyperbranched styrenic polymer with AB monomer bearing a nitroxide group. Besides AB monomers, an AB chain transfer agent (CTA) having chain transfer group B was reported for preparation of hyperbranched poly(methyl methacrylate) (PMMA) and its styrene block copolymer through reversible addition–fragmentation chain transfer (RAFT) polymerization.²² In addition, AB-type monomers having two vinyl groups with different reactivity were also used to prepare hyperbranched acrylic polymers by RAFT polymerization.²³ New approaches other than SCVP, such as “click” chemistry of AB₂ monomer, were also attempted.^{1,24} However, design and synthesis of AB monomers or compounds were complicated.

Using conventional free radical polymerization, Sherrington et al.^{25–29} found that hyperbranched PMMA samples could be readily synthesized through copolymerization of MMA with a di- or multivinyl monomer in the presence of a chain transfer agent (CTA) such as mercaptan. The di- or multivinyl monomer acted as a branching agent (BA) with cross-linking reaction suppressed by the CTA. This approach was later extended to various vinyl and divinyl monomer systems with group transfer copolymerization,³⁰ ATRP^{30–41} and RAFT polymerization.^{10,41–47} In ATRP polymerization, the ratios of initiator to BA > 1 were used in order to minimize gelation.^{30–41} A large amount of CTAs with CTA/BA ratios > 0.5 were often required in conventional free radical polymerization^{25–29} or RAFT polymerization^{10,41–47} to sufficiently control cross-linking reaction. Nevertheless, it is desirable in industrial practice that hyperbranched polymers are produced at low CTA loading and high monomer conversion.

In this paper, we report the synthesis of hyperbranched polyacrylamide (b-PAM) via a semibatch RAFT polymerization process with *N,N'*-methylenebis(acrylamide) (BisAM) as BA and 3-benzyltrithiocarbonyl propionic acid (BCPA) as CTA. Low CTA levels with BCPA to BisAM ratios < 0.05 were used in the work. Employing the semibatch process with the continuous

*Corresponding authors. (W.-J.W.) Telephone: +86-571-8795-2772. Fax: +86-571-8795-2772. E-mail: wenjunwang@zju.edu.cn. (S.Z.) Telephone: +1-905-525-9140 ext 24962; Fax: +1-905-521-1350. E-mail: zhuship@mcmaster.ca.

Scheme 1. Synthetic Route of Hyperbranched Polyacrylamide (b-PAM) Using Semi-Batch Reversible Addition–Fragmentation Chain Transfer (RAFT) Copolymerization of Acrylamide with *N,N'*-Methylenebisacrylamide (BisAM)



feeding of BisAM, the instantaneous BisAM concentration in the polymerization system could be controlled at a relatively low level, resulting high instantaneous ratio of CTA to BisAM to effectively suppress cross-linking reaction. The b-PAM samples were determined by gel permeation chromatography (GPC) equipped with differential refractive index (RI), viscometer (IV), and light scattering (LS) triple detectors. The samples were also characterized by NMR measurements. Branching density (BD) and distribution as well as cyclization density (CD) of the polymer samples were studied.

Experimental Section

Materials. Acrylamide (AM, $\geq 98.5\%$) was purchased from Lingfeng Chemical Reagent Co. Ltd., China. Ammonium persulfate (APS, $\geq 98\%$) and *N,N'*-methylenebis(acrylamide) (BisAM, $\geq 98\%$) were obtained from Sinopharm Chemical Reagent Co. Ltd., China. AM and BisAM were recrystallized in acetone and ethanol respectively before use, while APS was used as received. 3-Benzyltrithiocarbonyl propionic acid (BCPA) was synthesized according to the literature.⁴⁸

Synthesis of b-PAM by Semibatch RAFT Polymerization. The semibatch RAFT polymerization was used to produce b-PAMs as shown in Scheme 1. Divinyl monomer BisAM was continuously fed into the reaction system at a constant rate during polymerization. At the beginning, 7.1 g AM (0.1 mol), 100 g sodium acetate/acid acetate buffer solution at pH = 5, and 0.0453 g of chain transfer agent BCPA (1.67×10^{-4} mol) were added into a flask equipped with a mechanical stirrer. A certain amount of BisAM (0.513–1.540 g or 0.003–0.010 mol) was dissolved in 50 g of deionized water, and was inhaled in a syringe equipped to a micrometering pump. After N_2 was bubbled through for at least 30 min, the polymerization system was heated to 60 °C. The initiator APS (0.0130–0.0380 g or 5.70 – 16.67×10^{-5} mol) was injected to the flask to initiate polymerization. The BisAM solution was then fed to the system at a constant rate. After completion of BisAM addition, the polymerization was continued at 60 °C for another 30 min, prior to termination by cooling. The polymer samples were precipitated in ethanol, dried under vacuum, and further dialyzed for 7 days in a Spectra/Por dialysis membrane with molecular weight cutoff of 1000 g/mol.

Characterization. The b-PAM samples were characterized using a Polymer Laboratory PL-GPC 50 gel permeation chromatography (GPC) with differential refractive index (RI), viscometer (IV), and laser light scattering (LS) triple detectors. The detectors were installed in a series of LS, RI, and IV. For LS, the detection angle was 90° and the laser wavelength was 650 nm. A set of three columns of PL-aquagel-60, PL-aquagel-40, and PL-aquagel-30 were equipped in the GPC. 0.1N $NaNO_3$ aqueous solution was used as eluent at a flow rate 0.8 mL/min and 30 °C. PEO standards ($MW_1 = 1\,190\,000$ g/mol, $PDI_1 = 1.21$; $MW_2 = 162\,000$ g/mol, $PDI_2 = 1.45$; $MW_3 = 89\,000$ g/mol, $PDI_3 = 1.26$; $MW_4 = 600$ g/mol, $PDI_4 = 1.06$; as well as a PEO mixed standard having MW from 2000 to 162 000 g/mol) were used for calibrations. The dn/dc values for PAM and PEO were 0.170 and 0.133 mL/g, respectively.⁴⁹

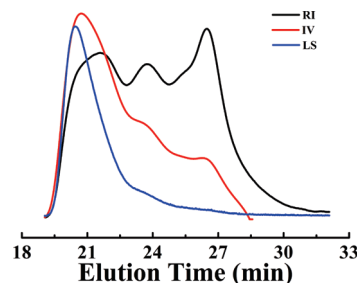


Figure 1. GPC traces from differential refractive index, viscometer, and laser light scattering detectors for the b-PAM sample of run 2.

which were measured using various PAM and PEO samples at different concentrations. The delay volumes IDD between the detectors were determined by PEO standards with 0.110 mL for LS and -0.562 mL for IV. Figure 1 shows typical GPC traces from RI, IV, and LS detectors (run 2 sample). 1H and ^{13}C NMR spectra were recorded on a Bruker Advance 400 MHz spectrometer with D_2O as solvent.

Results and Discussion

Table 1 provides a summary of polyacrylamide (PAM) samples synthesized by the semibatch RAFT copolymerization of AM with BisAM. All the samples except for those in runs 3 and 8 were soluble. Their weight-average molecular weight (M_w) were between $(5.63$ – $12.8) \times 10^5$ g/mol and polydispersity indexes (PDI) were between 4.7–8.6. The total monomer conversion was up to 96.1%. Linear PAMs as reference were also synthesized at various reaction times using the same recipe but in the absence of BisAM. The synthesis and characterization of linear PAM samples were supplied in the Supporting Information. The linear PAM sample after 4.5 h of polymerization had $M_w 7.95 \times 10^4$ g/mol and PDI 1.1 at the conversion 97.0%. The weight-average molecular weight was at least one-order of magnitude lower than that in the presence of BisAM, suggesting that branching did occur in the semibatch RAFT copolymerization of AM and BisAM. The GPC traces from viscometer (IV) and light scattering (LS) detectors for run 2 sample (Figure 1) showed strong responses at low elution time (i.e., high molecular weight fraction) and further supported b-PAM.

The b-PAM samples were characterized with an NMR spectrometer. Figure 2 shows 1H and ^{13}C NMR spectra for the run 5 sample. In the 1H NMR spectrum, the peaks at 6.8 and 7.5 ppm were the pendant double bonds of BisAM with one vinyl reacted. The content of residual (unreacted) pendant double bonds (c_p) was about 0.58–2.23% of the total reacted vinyl groups (from both reacted AM and reacted BisAM), suggesting that not all reacted BisAM contributed to branching. Using eq A8 (see Appendix), the fractions of pendent double bonds over the total incorporated BisAM (f_p) having one or both vinyl groups reacted were estimated and listed in Table 2. The detail for the calculation

Table 1. Synthesis and Characterization of Hyperbranched Polyacrylamides (b-PAMs) Using Semi-Batch RAFT Copolymerization ^a

run	AM, ^b wt %	[BisAM] ₀ / [CTA] ₀	[CTA] ₀ /[I] ₀	<i>r_a</i> , ^c mL/h	<i>x</i> , ^d %	<i>M_w</i> × 10 ⁻⁴ , g/mol	PDI	[η], dL/g	<i>c_p</i> , ^e %	<i>g</i> ^f	<i>g'</i>
1	4.7	20	2	16.7	91.3	57.0	5.1	0.712	0.74	0.416	0.288
2	4.7	30	2	16.7	95.2	128	8.4	0.892	0.94	0.301	0.210
3	4.7	50	2	16.7	gel						
4	4.7	30	2	33.3	83.1	121	8.6	0.799	0.58	0.295	0.201
5	4.7	30	2	11.1	93.5	58.2	5.3	0.701	2.23	0.411	0.290
6	4.7	30	3	16.7	73.1	56.8	4.7	0.605	1.00	0.359	0.256
7	5.7	30	2	16.7	92.7	56.3	4.8	0.691	1.40	0.409	0.280
8	7.1	30	2	16.7	gel						
9 ^g	4.7	30	2	16.7	96.1	124	7.8	0.878	0.93	0.306	0.216

^a Initial acrylamide concentration [AM]₀ was 1 mol/L. BCPA and APS were used as CTA and initiator, respectively. [AM]₀/[CTA]₀ was kept at 600/1 for all runs. All runs were carried out in buffer solutions of pH = 5 at 60 °C. ^b Weight percent of AM in total solvent. Various concentrations were achieved by changing amount of water in feeding BisAM solution. ^c *r_a*: feeding rate of BisAM solution. ^d *x*: total monomer conversion. ^e *c_p*: molar ratio of pendant double bond to polymerized vinyl units calculated from ¹H NMR spectra. ^f *g'* and *g* were weight-average contraction factors. ^g Repeated run with the same experimental condition as in run 2 with extension of polymerization time after the BisAM feeding from 0.5 to 2 h.

was elaborated in the Appendix. The results showed that about 52–89% of the incorporated BisAM monomers had both vinyl groups reacted contributing to either branching or cyclization.

Branched polymer chains show stronger shrinking effect than their linear counterparts.^{2,24,50} They have lower root mean-square gyration radius $\langle R_g^2 \rangle^{1/2}$ and intrinsic viscosity $[\eta]$.⁵¹ The level of branching density can be described by the contraction factors *g* and *g'* as

$$g = \frac{\langle R_g^2 \rangle_{br}}{\langle R_g^2 \rangle_{lin}} \quad (1)$$

$$g' = \frac{[\eta]_{br}}{[\eta]_{lin}} \quad (2)$$

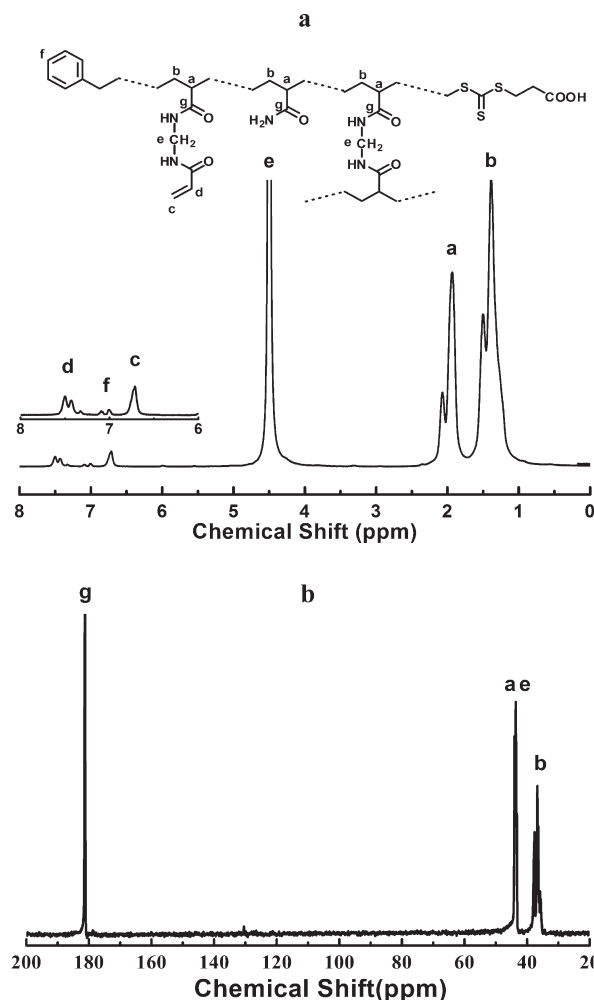
From five linear PAM reference samples (*MW*₁ = 4.76 × 10⁴ g/mol, *PDI*₁ = 1.04; *MW*₂ = 6.59 × 10⁴ g/mol, *PDI*₂ = 1.11; *MW*₃ = 7.47 × 10⁴ g/mol, *PDI*₃ = 1.15; *MW*₄ = 7.85 × 10⁴ g/mol, *PDI*₄ = 1.15, and *MW*₅ = 1.07 × 10⁶ g/mol, *PDI*₅ = 1.55), the following Mark–Houwink equation was found: $[\eta] = 1.12 \times 10^{-4} M^{0.769}$. The M–H parameters agreed with those reported in the *Polymer Handbook*.⁴⁹ Applying Fox–Flory correlation gave $\langle R_g^2 \rangle^{1/2} = 1.70 \times 10^{-2} M^{0.583}$.^{52,53} The *g* and *g'* data for the soluble b-PAM samples are listed in Table 1, with *g'* in the range of 0.295–0.416 and *g* in the range 0.201–0.290. The polymers having higher branching densities clearly gave lower *g'* and *g* values at the same molecular weight.

The following quantitative relationship existed between *g* and *g'*,

$$g' = g^\varepsilon \quad (3)$$

where ε is an exponential factor. From the *g* and *g'* data in Table 1, the ε value for the b-PAM samples was determined to be 0.74. The ε value was used for further estimation of branching density from *g'*.

Molecular Weight Dependence of Branching Density and Distribution in b-PAM. The $[\eta]$ versus molecular weight correlations for the soluble b-PAM samples are presented in Figure 3. The molecular weight values in the figure were those corresponding to their GPC elution fractions. The linear PAM data are also included in Figure 3 as reference. All the $[\eta]$ values of b-PAMs were substantially lower than their linear counterparts. Using eq 2, we calculated the contraction factor *g'*, i.e., the $[\eta]$ ratio of b-PAM over linear PAM at the same molecular weight. The estimated *g'* values are plotted against molecular weight in Figure 4. Figure 4a also gives a plot of the *g'* overlaid with its GPC trace for run 2 sample. The figures of *g'* values overlaid with their GPC traces for the rest b-PAM samples are presented in the

**Figure 2.** (a) ¹H NMR and (b) ¹³C NMR spectra of b-PAM sample of run 5.

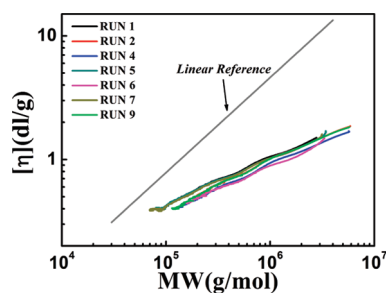
Supporting Information. It shows each GPC elution fraction for all the b-PAM samples had the $[\eta]$ and *g'* values determined by *f_p*. The curves of $[\eta] \sim M$ and *g'* $\sim M$ for runs 4 and 6 (*f_p* = 10.5–21.7%) were the lowest, while those of runs 2 and 9 (*f_p* = 19.4–20.4%) in the middle, and runs 5 and 7 (*f_p* = 28.1–48.0%) further increased, with run 1 the highest due to lowest usage of BisAM.

As the reactivity ratios of BisAM and AM are close to 1,^{54,55} the branched structures in the b-PAMs are expected to be distributed randomly along primary chain backbones. The BisAM serves as a bridge to connect two primary chains

Table 2. Branching Densities, Cyclization Densities, and Fractions of BisAM Contributed to Their Formation Determined by ^1H NMR, GPC with Triple-Detector, and Fractionation of GPC Traces for b-PAMs

run	$[\text{BisAM}]_0/[\text{AM}]_0$	$\text{BD}_{\text{GPC}}, \text{C}/1000\text{C}$	$\text{BD}_{\text{ps}},^a \text{C}/1000\text{C}$	$\text{CD}_{\text{NMR}},^b \text{C}/1000\text{C}$	$f_p,^c \%$	$f_{br},^c \%$	$f_{cyc},^c \%$
1	3.3/100	7.2	7.5	16.5–19.4	23.6–21.6	23.2–21.2	53.2–57.3
2	5.0/100	9.6	9.6	26.6–28.9	20.4–19.4	21.2–20.1	58.4–60.4
4	5.0/100	11.7	11.9	28.0–37.3	12.6–10.5	25.8–21.4	61.6–68.1
5	5.0/100	7.5	8.4	16.2–19.3	48.0–44.9	16.5–15.4	35.6–39.8
6	5.0/100	11.5	11.7	24.1–41.0	21.7–15.8	25.3–18.5	52.9–65.7
7	5.0/100	7.7	8.6	23.9–27.6	30.4–28.1	16.9–15.7	52.7–56.2
9	5.0/100	9.5	9.7	26.7–28.6	20.2–19.4	21.0–20.2	58.8–60.4

^a BD estimated from fractionation of GPC curves. ^b CD estimated from the amount of polymerized BisAM contributed to cyclization in b-PAMs using eq A7 with min to max range. ^c f_p , f_{br} , and f_{cyc} are fractions of reacted BisAM contributed to pendent double bonds, branches, and cyclic structures calculated by eqs A8–A10. The ranges of f_p , f_{br} , and f_{cyc} are estimated based on min and max CD values.

**Figure 3.** Intrinsic viscosity as a function of molecular weight of GPC elution fraction of b-PAM samples.

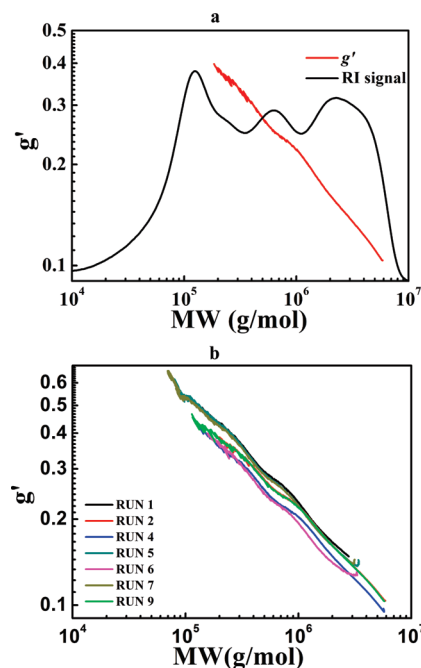
(counted as two carbons in one branch for density estimation), giving an H-type structure. Hence, we can apply Zimm-Stockmayer equation⁵¹ to estimate the branching frequency (BF, carbons per polymer molecule) and branching density (BD, carbons per 1000 carbons).

$$g = \left[\left(\sqrt{1 + \left(\frac{\text{BF}}{6} \right)} \right) + \frac{4 \times \text{BF}}{3\pi} \right]^{-1/2} \quad (4)$$

$$\text{BD} = \frac{35\,500 \times \text{BF}}{M} \times 2 \quad (5)$$

where the g data were obtained through converting g' in Figure 4 using eq 3. Figure 5 shows the BF and BD results. By an average, polymer molecules having molecular weight 10^5 g/mol contained approximately 10 to 15 branches, and those of $\text{MW} = 10^6$ g/mol had 110 to 200 branches. The BD values for runs 1, 5, and 7 were 6–11 C/1000C, while runs 2 and 9 were 9–13 C/1000C, and runs 4 and 6 were 11–16 C/1000C.

The average BDs for the b-PAM samples can be calculated from $\sum_i \text{BD}_i C_i / \sum_i C_i$, where C_i is the polymer concentration at each GPC elution fraction. These BD values are summarized in Table 2. The b-PAM samples had average BDs from 7.2 to 11.7 C/1000C. It was found that the BD values were substantially lower than those estimated by assuming all incorporated BisAM with both vinyl groups reacted contributed to branching, suggesting some of the incorporated BisAM formed the cyclic structures during the polymerization. The same observation was made in other vinyl and divinyl monomer RAFT polymerization systems.^{42,44,47} On the basis of the BD and c_p values, the cyclization densities (CD, carbons per 1000 carbons) in the b-PAM samples were calculated using eq A7, as shown in Table 2. The b-PAM samples had CD values of 16.2–48.0 C/1000C. The CD values were substantially higher than BDs. To quantify the relative contributions of the reacted BisAM to branching and cyclization, their fractions, f_{br} and f_{cyc} , were estimated

**Figure 4.** (a) Contraction factor g' overlaid with GPC trace of the run 2 sample and (b) g' of b-PAM samples as a function of molecular weight of GPC elution fraction.

using eqs A9 and A10, and summarized in Table 2. The f_{cyc} values were 35.6–68.1% compared with 15.4–25.8% of f_{br} , reflecting that approximately half of the reacted BisAM participated in the formation of cyclic structures, and 1/6–1/4 contributed to branching. The intramolecular cyclization reactions were more competitive than intermolecular branching during the polymerization.

Fractionation of GPC Traces for b-PAMs. A randomly branched polymer has a branch-on-branch structure and can be considered as an aggregation of linear chains at branch points. In general, a branched chain consisted of i primary linear chains.⁵⁶ Because of high branching densities, the b-PAM samples contained a large number of primary chains. The theoretical molecular weight of the primary chain was estimated from the ratio of monomer to CTA, for example, 4.5×10^4 g/mol in run 2. The experimental molecular weight of 6.2×10^4 g/mol was used for fractionation of run 2. The molecular weight of the i -chain was i times of the primary chain. The molecular weight distribution of the primary chain was assumed to follow a Gaussian function, based on the experimental observation of AM polymerization. The multipeak molecular weight distribution of the b-PAM samples could then be fractionated into several sub population of i -chains. Figure 6 shows an example of the fractionation of GPC trace for run 2. The weight fractions $\omega(i)$ of

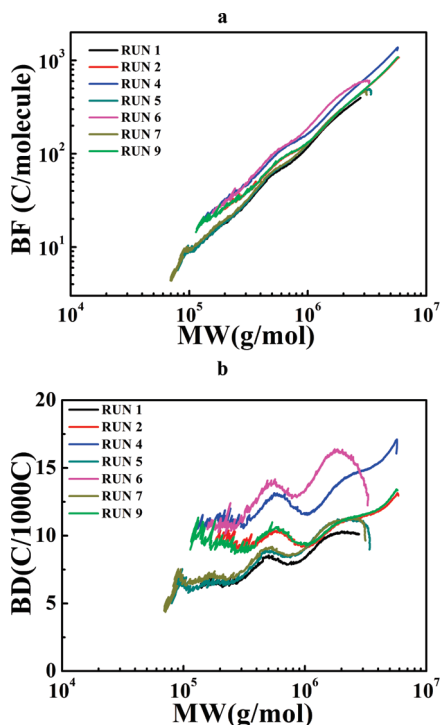


Figure 5. Branching frequency (a, BF) and branching density (b, BD) as a function of molecular weight of GPC elution fraction for b-PAM samples.

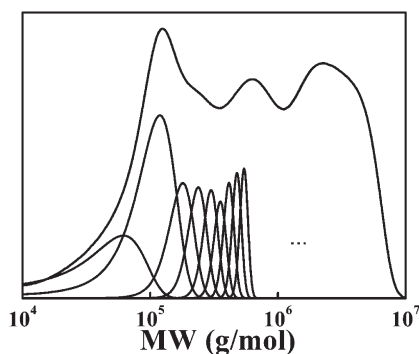


Figure 6. Fractionation of GPC trace of b-PAM sample of run 2 on the basis of i number of primary chain ($i = 1, 2, 3, 4, \dots$).

i -chains were estimated by optimized curve fitting, as shown in Figure 7.

The characteristic feature of the $\omega(i)$ versus i curves was similar to the theoretical distribution for randomly branched polymers.⁵⁶ Using the branching frequencies (BF) at various molecular weights in Figure 5a, the BF values corresponding to i -chains were estimated. Dividing these BF values by i gave the BF per primary chain, as shown in Figure 8. It can be seen that each primary chain in the b-PAM samples had similar level of branching densities, indicating the b-PAM samples had relatively uniform random-branched distribution. The average BDs estimated from $\sum \omega(i)(35\,500\text{BF}_i/M_i) \times 2$ were summarized in Table 2. A good agreement of the BD values from both GPC and peak fractionation further supported the uniform distribution of random branches in the b-PAM samples.

Effect of BisAM/CTA Ratio. Highly branched structures can be achieved by increasing divinyl monomer concentration. However, there is a risk of gelation through cross-linking reaction. A high CTA level with BisAM/CTA ratio < 2 was used in the batch polymerization to suppress cross-linking

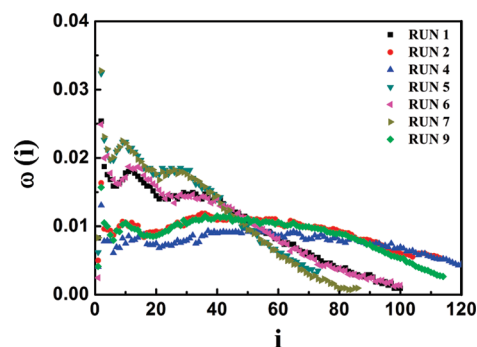


Figure 7. Weight fraction $\omega(i)$ distribution of i -chains in b-PAM samples using the fractionation of GPC trace in Figure 6.

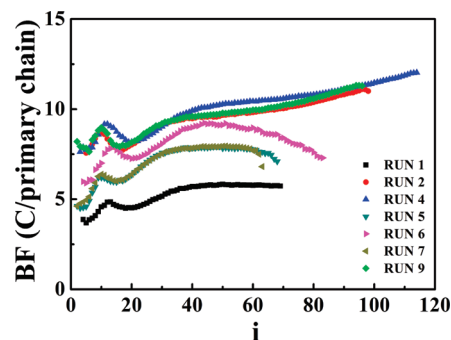


Figure 8. Branching frequency of i -chains in b-PAM samples.

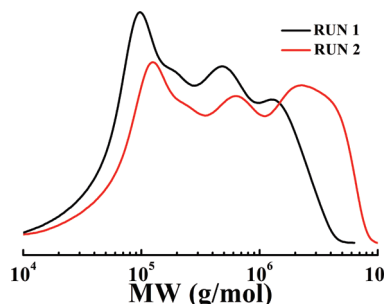


Figure 9. GPC traces of b-PAM samples of runs 1 and 2 prepared by semibatch RAFT copolymerization of AM with different ratios of BisAM at pH = 5, 60 °C, $[\text{AM}]_0 = 1 \text{ mol/L}$, $[\text{AM}]_0/[\text{CTA}]_0/[I]_0 = 600/1/0.5$, and 16.7 mL/h of BisAM feeding rate. Run 1: $[\text{BisAM}]_0/[\text{CTA}]_0 = 20$. Run 2: $[\text{BisAM}]_0/[\text{CTA}]_0 = 30$.

reaction.^{10,25–29,41–47} Using the semibatch polymerization operation with continuous feeding of BisAM, b-PAMs were successfully prepared at high BisAM/CTA ratios (e.g., 30 in run 2). The CTA concentrations in this study were at least 15 times lower than those reported in the literatures.^{10,25–29,41–47} This is because the continuous BisAM feeding mode could control the instantaneous BisAM concentration at a relatively low level. Therefore, high instantaneous ratio of CTA to BisAM in current polymerization system was achieved to effectively control the gelation. Further increase of BisAM ratio will increase instantaneous divinyl monomer concentration, thus lowering instantaneous ratio of CTA to BisAM. When the overall BisAM/CTA ratio was increased to 50 (run 3), that is the BisAM/AM ratio of 8.3/100 was utilized, the amount of CTA in the polymerization system was not sufficient to suppress the cross-linking reaction. The system was thus gelled in 97 min.

Figure 9 shows the GPC traces of b-PAM samples at BisAM/CTA of 20 (run 1) and 30 (run 2). When the ratio was

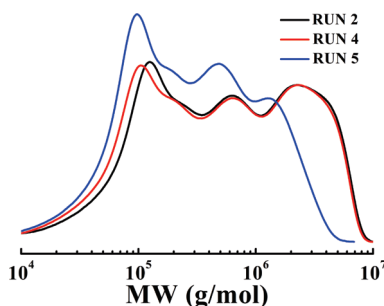


Figure 10. GPC traces of b-PAM samples of runs 2, 4, and 5 with different BisAM feeding rate (r_a), pH = 5, 60 °C, $[AM]_0 = 1$ mol/L, and $[AM]_0/[BisAM]_0/[CTA]_0/[I]_0 = 600/30/1/0.5$. Run 4: $r_a = 33.3$ mL/h. Run 2: $r_a = 16.7$ mL/h. Run 5: $r_a = 11.1$ mL/h.

increased from 20 to 30 at the same initial CTA concentration ($[CTA]_0/[AM]_0 = 1:600$), equivalent to change of the BisAM/AM ratio from 3.3/100 to 5/100, a higher BisAM concentration thus existed in run 2. The fraction of polymer chains between 10^6 and 10^7 g/mol increased. The average molecular weight (M_w) increased from 5.70×10^5 to 1.28×10^6 g/mol and PDI from 5.1 to 8.4. Both run 2 and 3 had about 21% of polymerized BisAM contributing to branching with more cyclization structures existed in run 2 (CD = 26.6–28.9) than those in run 1 (CD = 16.5–19.4). The fraction of polymerized BisAM participating cyclization (f_{cyc}) in run 2 was higher than that in run 1, indicating high divinyl monomer concentration in favor of forming cyclic structures. The g' decreased from 0.416 to 0.301 while the g from 0.288 to 0.210. More branches were formed in run 2 (BD of 9.6 C/1000C) than in run 1 (7.5 C/1000C).

Effect of BisAM Feeding Rate. The BisAM concentration in the polymerization system can be adjusted by feeding rate. The control of instantaneous BisAM concentration was actually the key to the success of hyperbranched structure formation at low CTA levels in this study. Three addition rates (r_a) of 33.3 mL/h (run 4), 16.7 mL/h (run 2), and 11.1 mL/h (run 5) were used to feed the same amount of BisAM. Although the lowest monomer conversion of 83.1% was obtained in run 4 due to its shortest polymerization time (corresponding to the highest feeding rate), the highest branching density was achieved with the BD of 11.7 C/1000C. The g' and g had the lowest values of 0.295 and 0.201, respectively. This was because of the highest instantaneous BisAM concentration and thus the highest fraction of the reacted BisAM 21.4–25.8% contributing to branching. The high instantaneous BisAM concentration also promoted the formation of cyclic structures at the mean time. The CD were 28.0–37.3 C/1000C with f_{cyc} of 61.6–68.1% in run 4. When r_a was reduced to 11.1 mL/h, the BD became 8.4 C/1000C and less reacted BisAM (15.4–16.5%) contributed to branching. The g' and g values changed to 0.411 and 0.290, respectively. The sample had lowest CD of 16.2–19.3 C/1000C. But more BisAM had only one vinyl group consumed with the f_p increased to 44.9–48.0%. The polymer sample produced in run 4 had M_w of 1.21×10^6 g/mol and PDI of 8.6, a similar high molecular weight range of 10^6 – 10^7 g/mol to run 2, and slight difference in the low molecular weight range as shown in Figure 10. The M_w of the polymer synthesized with BisAM feeding rate of 11.1 mL/h (run 5) decreased to 5.82×10^5 g/mol with PDI of 5.3. More branched structures formed at faster BisAM feeding further support the instantaneous ratio of CTA to BisAM concentration is key to branching formation and gelation control. Although less cyclic structures were generated at low instantaneous BisAM concentration, which is consistent with the

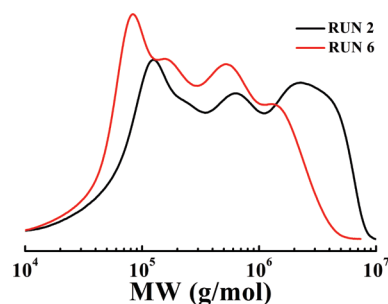


Figure 11. GPC traces of b-PAM samples of runs 2 and 6 at different $[CTA]_0/[I]_0$, pH = 5, 60 °C, $[AM]_0 = 1$ mol/L, $[AM]_0/[BisAM]_0/[CTA]_0 = 600/30/1$, and 16.7 mL/h of BisAM feeding rate. Run 2: $[CTA]_0/[I]_0 = 2$. Run 6: $[CTA]_0/[I]_0 = 3$.

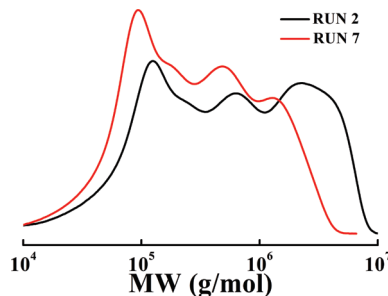


Figure 12. GPC traces of b-PAM samples of runs 2 and 7 at different overall AM concentrations, pH = 5, 60 °C, $[AM]_0 = 1$ mol/L, $[AM]_0/[BisAM]_0/[CTA]_0/[I]_0 = 600/30/1/0.5$, and 16.7 mL/h of BisAM feeding rate. Run 2: 4.7 wt % AM in total solvent. Run 7: 5.7 wt %.

observation in the study of different BisAM/CTA ratio effect, the control of low instantaneous BisAM concentration was not in favor of branching.

Effect of Initiator Concentration. When the initiator concentration in run 6 was lowered to 2/3 of the amount in run 2, the polymerization rate was influenced. The overall monomer conversion decreased from 95.2% to 73.1%. However, the BD in run 6 was 11.5 C/1000C, higher than 9.6 C/1000C in run 2, due to more BisAM contributing to branching. The run 6 sample had g' of 0.359 and g of 0.256, higher than those in run 2. The discrepancy was because of the molecular weight of run 2 sample substantially higher than that of run 6, and having more significant contribution from the molecular weight fraction of less than 10^6 g/mol in run 6 than in run 2, as shown in Figure 11.

Effect of AM Concentration. The polymerization systems at three AM concentration levels of 4.7% (run 2), 5.7% (run 7), and 7.1% (run 8) were investigated. Soluble b-PAM samples were obtained with 4.7% and 5.7%. When the AM level increased to 7.1% (run 8), gelation occurred in 75 min, suggesting high solid content in favor of cross-linking reactions. Compared to run 2 (4.7%), the polymer sample of run 7 (5.7%) was less branched. The BD of run 7 was 7.7 C/1000C. The g' and g were 0.409 and 0.280, respectively. Lower BD in run 7 was mainly due to about 10% more BisAM having only one vinyl group reacted than that in run 2, with less reacted BisAM contributed to branching. Less cyclic structures in run 7 was also found, which is in good agreement with the observation of low polymer concentration favoring intramolecular cyclization in RAFT copolymerization of 2-aminoethyl methacrylate with a disulfide-based dimethacrylate.⁴² The run 7 sample had a lower molecular weight than run 2 as shown in Figure 12. There was a larger fraction of chains having molecular weight $< 10^6$ g/mol in run 7 than in run 2.

Conclusions

Hyperbranched polyacrylamides (b-PAM) were synthesized using a semibatch RAFT copolymerization of acrylamide (AM) and *N,N'*-methylenebis(acrylamide) (BisAM) in the presence of chain transfer agent (CTA) of BCPA with continuous feeding of BisAM. The cross-linking reaction of BisAM was effectively suppressed even at a low CTA to BisAM ratio of 1/30. This is mainly due to low instantaneous BisAM concentration in polymerization system sustained by using the semibatch process, thus maintaining sufficiently high instantaneous ratio of CTA to BisAM to minimize the gelation. The b-PAM samples had weight-average molecular weights in the range $(5.63\text{--}12.8) \times 10^5$ g/mol and polydispersity indexes of 4.7–8.6. The GPC measurement with online differential refractive index, viscometer, and laser light scattering detectors showed that the b-PAM samples had branching densities of 7.2–11.7 carbons per 1000 carbons, with contraction factors g' of 0.295–0.416 and g of 0.201–0.290. Fractionation of the GPC traces of *i*-chains elucidated that the b-PAM samples had branches randomly distributed along primary chains. It was also found the intramolecular cyclization reactions were more competitive than intermolecular branching during the polymerization. Less than a quarter of reacted BisAM molecules contributed to the branched structures while approximately half of the reacted BisAM formed cyclic structures. Lower instantaneous BisAM concentration in the polymerization system via using lower BisAM/CTA ratio or higher BisAM feeding rate favored less cyclic structures generated, but lessened branching formation. Samples having high branching densities but little gel content were achieved with high BisAM to CTA molar ratio $([\text{BisAM}]_0/[\text{CTA}]_0 = 30:1)$, fast feeding of BisAM ($r_a = 33.3$ mL/h), and low monomer concentration level in aqueous solution (4.7 wt %).

Acknowledgment. This work is financially supported by the Zhejiang Ministry of Science and Technology (Strategic Grant, No. 2008C14087), the National Natural Science Foundation of China (Key Grant, No. 20936006), and the Chinese State Key Laboratory of Chemical Engineering at Zhejiang University (Grant No. SKL-ChE-08D01). W.-J.W. also thanks the Macromolecule and Renewable Resource Research Platform of Zhejiang University funded by Chinese National 985 Program for a Start-up Fund.

Appendix

Calculation of Fractions of BisAM Contributing to Branch (f_{br}), Pendent Vinyl Group (f_p), and Cyclic Structure (f_{cyc}), as Well as Cyclization Density (CD). The molar ratio of pendant vinyl to total reacted vinyl in the polymer (c_p) can be determined from ^1H NMR spectra and expressed as follows,

$$c_p = \frac{m_{\text{BisAM},p}}{m_{\text{AM}} + 2m_{\text{BisAM}} - m_{\text{BisAM},p}} \quad (\text{A1})$$

where m_{BisAM} and m_{AM} are the moles of BisAM and AM incorporated into the polymer, respectively, $m_{\text{BisAM},p}$ is the mole of BisAM with one vinyl reacted and the other pendant in the polymer. Therefore,

$$m_{\text{BisAM},p} = \frac{c_p(m_{\text{AM}} + 2m_{\text{BisAM}})}{1 + c_p} \quad (\text{A2})$$

The m_{BisAM} and m_{AM} can be calculated from their individual conversions of x_{BisAM} and x_{AM} and initial moles of $m_{\text{BisAM},0}$ and $m_{\text{AM},0}$.

$$m_{\text{BisAM}} = m_{\text{BisAM},0}x_{\text{BisAM}} \quad (\text{A3})$$

$$m_{\text{AM}} = m_{\text{AM},0}x_{\text{AM}} \quad (\text{A4})$$

The overall conversion x can be correlated to x_{BisAM} and x_{AM} as

$$x = \frac{x_{\text{BisAM}} \frac{m_{\text{BisAM},0}}{m_{\text{AM},0}} \frac{mw_{\text{BisAM}}}{mw_{\text{AM}}} + x_{\text{AM}}}{\frac{m_{\text{BisAM},0}}{m_{\text{AM},0}} \frac{mw_{\text{BisAM}}}{mw_{\text{AM}}} + 1} \quad (\text{A5})$$

where mw_{BisAM} and mw_{AM} are molecular weights of BisAM and AM, respectively.

As $m_{\text{BisAM},0}/m_{\text{AM},0} = [\text{BisAM}]_0/[\text{AM}]_0$, let $r_m = [\text{BisAM}]_0/[\text{AM}]_0$ and $r_{mw} = mw_{\text{BisAM}}/mw_{\text{AM}}$, and we have

$$x_{\text{AM}} = x(r_m r_{mw} + 1) - x_{\text{BisAM}} r_m r_{mw} \quad (\text{A6})$$

Note there are two methine carbons in a cyclic structure. From the above equations, the cyclization density (CD) can be determined by

$$\begin{aligned} \text{CD} &= \frac{m_{\text{BisAM}} - m_{\text{BisAM},p}}{2m_{\text{BisAM}} + m_{\text{AM}}} \times 1000 - \text{BD} \\ &= \frac{r_m - c_p \left(\frac{x_{\text{AM}}}{x_{\text{BisAM}}} + 2r_m \right) / (1 + c_p)}{2r_m + \frac{x_{\text{AM}}}{x_{\text{BisAM}}}} \times 1000 - \text{BD} \quad (\text{A7}) \end{aligned}$$

where branching density (BD, carbons per 1000 carbons) is determined from GPC. Previous studies^{54,55} showed that the reactivity ratios of BisAM and AM were close to 1 with BisAM slightly more reactive. In addition, low BisAM concentration was maintained during the polymerization due to continuous feeding of BisAM. Hence, the x_{BisAM} was larger than the x_{AM} . The minimum x_{BisAM} value was the overall conversion x while the maximum x_{BisAM} could reach 1. Both values were used for the calculation of CD_{NMR} in Table 2.

The fractions of BisAM contributing to pendent vinyl group (f_p), branch (f_{br}), and cyclization structure (f_{cyc}) can be respectively estimated from

$$f_{\text{pend}} = \frac{m_{\text{BisAM},p}}{m_{\text{BisAM}}} = \frac{c_p \left(\frac{x_{\text{AM}}}{x_{\text{BisAM}} r_m} + 2 \right)}{1 + c_p} \quad (\text{A8})$$

$$\begin{aligned} f_{br} &= \frac{m_{\text{BisAM}} - m_{\text{BisAM},p}}{m_{\text{BisAM}}} \times \frac{\text{BD}}{\text{BD} + \text{CD}} \\ &= \left(1 - \frac{c_p \left(\frac{x_{\text{AM}}}{x_{\text{BisAM}} r_m} + 2 \right)}{1 + c_p} \right) \times \frac{\text{BD}}{\text{BD} + \text{CD}} \quad (\text{A9}) \end{aligned}$$

$$f_{cyc} = 1 - f_{\text{pend}} - f_{br} \quad (\text{A10})$$

The f_{br} , f_p , and f_{cyc} values were estimated from both minimum and maximum CD_{NMR} in Table 2.

Supporting Information Available: Figures and text discussing monomer conversion, molecular weight and polydispersity index of linear PAM samples in RAFT homopolymerization, and g' plots overlaid with GPC traces for b-PAM samples. This material is available free of charge via the Internet at <http://pubs.acs.org>.

References and Notes

- (1) Konkolewicz, D.; Gray-Weale, A.; Perrier, S. *J. Am. Chem. Soc.* **2009**, *131*, 18075–18077.
- (2) Voit, B. I.; Lederer, A. *Chem. Rev.* **2009**, *109*, 5924–5973.
- (3) Sun, H. C.; Mu, S. J.; Soon, H. Y. *Eur. Polym. J.* **1999**, *35*, 1841–1845.
- (4) Housni, A.; Narain, R. *Eur. Polym. J.* **2007**, *43*, 4344–4354.
- (5) Plamper, F. A.; Schmalz, A.; Ballauff, M.; Müller, A. H. E. *J. Am. Chem. Soc.* **2007**, *129*, 14538–14539.
- (6) Campillo, C. C.; Schröder, A. P.; Marques, C. M.; Pépin-Donat, B. *Soft Matter* **2008**, *4*, 2486–2491.
- (7) Wei, H.; Cheng, S.-X.; Zhang, X.-Z.; Zhuo, R.-X. *Prog. Polym. Sci.* **2009**, *34*, 893–910.
- (8) Boyer, C.; Bulmus, V.; Davis, T. P.; Ladmiral, V.; Liu, J.; Perrier, S. *Chem. Rev.* **2009**, *109*, 5402–5436.
- (9) Peleshanko, S.; Tsukruk, V. V. *Prog. Polym. Sci.* **2007**, *33*, 523–580.
- (10) Liu, B.; Kazlauciusas, A.; Guthrie, J. T.; Perrier, S. *Macromolecules* **2005**, *38*, 2131–2136.
- (11) Hawker, C. J.; Fréchet, J. M. J.; Grubbs, R. B.; Dao, J. *J. Am. Chem. Soc.* **1995**, *117*, 10763–10764.
- (12) Sunder, A.; Hanselmann, R.; Frey, H.; Mulhaupt, R. *Macromolecules* **1999**, *32*, 4240–4246.
- (13) Jikei, M.; Kakimoto, M. *Prog. Polym. Sci.* **2001**, *26*, 1233–1285.
- (14) Fréchet, J. M. J.; Henmi, M.; Gitsov, I.; Aoshima, S.; Leduc, M. R.; Grubbs, R. B. *Science* **1995**, *269*, 1080–1083.
- (15) Matyjaszewski, K.; Pyun, J.; Gaynor, S. G. *Macromol. Rapid Commun.* **1998**, *19*, 665–670.
- (16) Matyjaszewski, K.; Gaynor, S. G.; Müller, A. H. E. *Macromolecules* **1997**, *30*, 7034–7041.
- (17) Matyjaszewski, K.; Gaynor, S. G. *Macromolecules* **1997**, *30*, 7042–7049.
- (18) Matyjaszewski, K.; Gaynor, S. G.; Kulfan, A.; Podwika, M. *Macromolecules* **1997**, *30*, 5192–5194.
- (19) Gaynor, S. G.; Edelman, S.; Matyjaszewski, K. *Macromolecules* **1996**, *29*, 1079–1081.
- (20) Yan, D. Y.; Müller, A. H. E.; Matyjaszewski, K. *Macromolecules* **1997**, *30*, 7024–7033.
- (21) Simon, P. F. W.; Radke, W.; Müller, A. H. E. *Macromol. Rapid Commun.* **1997**, *18*, 865–873.
- (22) Yamada, B.; Konosu, O.; Tanaka, K.; Oku, F. *Polymer* **2000**, *41*, 5625–5631.
- (23) Lin, Y.; Liu, X.; Li, X.; Zhan, J.; Li, Y. *J. Polym. Sci., Part A: Polym. Chem.* **2007**, *45*, 26–40.
- (24) Kong, L. Z.; Sun, M.; Qiao, H.-M.; Pan, C.-Y. *J. Polym. Sci., Part A: Polym. Chem.* **2010**, *48*, 454–462.
- (25) Slark, A. T.; Sherrington, D. C.; Titterton, A.; Martin, I. K. *J. Mater. Chem.* **2003**, *13*, 2711–2720.
- (26) Isaure, F.; Cormack, P. A. G.; Sherrington, D. C. *J. Mater. Chem.* **2003**, *13*, 2701–2710.
- (27) Isaure, F.; Cormack, P. A. G.; Sherrington, D. C. *Macromolecules* **2004**, *37*, 2096–2105.
- (28) Costello, P. A.; Martin, I. K.; Slark, A. T.; Sherrington, D. C.; Titterton, A. *Polymer* **2002**, *43*, 245–254.
- (29) O'Brien, N.; McKee, A.; Sherrington, D. C.; Slark, A. T.; Titterton, A. *Polymer* **2000**, *41*, 6027–6031.
- (30) Isaure, F.; Cormack, P. A. G.; Graham, S.; Sherrington, D. C.; Arms, S. P.; Büttin, V. *Chem. Commun.* **2004**, 1138–1139.
- (31) Wang, A. R.; Zhu, S. *Macromolecules* **2002**, *35*, 9926–9933.
- (32) Li, Y.; Arms, S. P. *Macromolecules* **2005**, *38*, 8155–8162.
- (33) Wang, A. R.; Zhu, S. *J. Polym. Sci., Part A: Polym. Chem.* **2005**, *43*, 5710–5714.
- (34) Wang, A. R.; Zhu, S. *Polym. Eng. Sci.* **2005**, *45*, 720–727.
- (35) Bannister, I.; Billingham, N. C.; Arms, S. P.; Rannard, S. P.; Findlay, P. *Macromolecules* **2006**, *39*, 7483–7492.
- (36) Bouhier, M.-H.; Cormack, P. A. G.; Graham, S.; Sherrington, D. C. *J. Polym. Sci., Part A: Polym. Chem.* **2007**, *45*, 2375–2386.
- (37) Yu, Q.; Qin, Z.; Li, J.; Zhu, S. *Polym. Eng. Sci.* **2008**, *48*, 1254–1260.
- (38) Yang, H.-J.; Jiang, B.-B.; Huang, W.-Y.; Zhang, D.-L.; Kong, L.-Z.; Chen, J.-H.; Liu, C.-L.; Gong, F.-H.; Yu, Q.; Yang, Y. *Macromolecules* **2009**, *42*, 5976–5982.
- (39) Li, W.; Gao, H.; Matyjaszewski, K. *Macromolecules* **2009**, *42*, 927–932.
- (40) Gao, H.; Matyjaszewski, K. *Prog. Polym. Sci.* **2009**, *34*, 317–350.
- (41) Yu, Q.; Xu, S.; Zhang, H.; Ding, Y.; Zhu, S. *Polymer* **2009**, *50*, 3488–3494.
- (42) Li, Y.; Arms, S. P. *Macromolecules* **2009**, *42*, 939–945.
- (43) Yu, Q.; Gan, Q.; Zhang, H.; Zhu, S. *ACS Symp. Ser.* **2009**, *1024*, 181–193.
- (44) Vo, C.-D.; Rosselgong, J.; Arms, S. P.; Billingham, N. C. *Macromolecules* **2007**, *40*, 7119–7125.
- (45) Poly, J.; Wilson, D. J.; Destarac, M.; Taton, D. *Macromol. Rapid Commun.* **2008**, *29*, 1965–1972.
- (46) Tao, L.; Liu, J.; Tan, B. H.; Davis, T. P. *Macromolecules* **2009**, *42*, 4960–4962.
- (47) Rosselgong, J.; Arms, S. P.; Barton, W.; Price, D. *Macromolecules* **2009**, *42*, 5919–5924.
- (48) Jesberger, M.; Barner, L.; Stenzel, M. H.; Malmstrom, E.; Davis, T. P.; Barner-Kowollik, C. *J. Polym. Sci., Part A: Polym. Chem.* **2003**, *41*, 3847–3861.
- (49) Brandrup, J.; Immergut, E. H.; Grulke, E. A.; Abe, A.; Bloth, D. R. *Polymer Handbook*, 4th ed.; John Wiley & Sons: New York, 1999.
- (50) Wang, W.-J.; Kharchenko, S.; Migler, K.; Zhu, S. *Polymer* **2004**, *45*, 6495–6505.
- (51) Zimm, B. H.; Stockmayer, W. H. *J. Chem. Phys.* **1949**, *17*, 1301–1314.
- (52) Fevola, M. J.; Bridges, J. K.; Kellum, M. G.; Hester, R. D.; McCormick, C. L. *J. Polym. Sci., Part A: Polym. Chem.* **2004**, *42*, 3236–3251.
- (53) Ezell, R. G.; Gorman, I.; Lokitz, B.; Ayres, N.; McCormick, C. L. *J. Polym. Sci., Part A: Polym. Chem.* **2006**, *44*, 3125–3139.
- (54) Nieto, J. L.; Baselga, J.; Hernandez-Fuentes, I.; Llorente, M. A.; Pierola, I. F. *Eur. Polym. J.* **1987**, *23*, 551–555.
- (55) Baselga, J.; Llorente, M. A.; Nieto, J. L.; Hernandez-Fuentes, I.; Pierola, I. F. *Eur. Polym. J.* **1988**, *24*, 161–165.
- (56) Zhu, S. *Macromolecules* **1998**, *31*, 7519–7527.